Journal of the Iranian Chemical Society
https://doi.org/10.1007/s13738-021-02287-9

ORIGINAL PAPER

Copper(II) sulfonamide complexes having enzyme inhibition activities on carbonic anhydrase I: synthesis, characterization and inhibition studies

Demet Uzun[1] · Ayla Balaban Gündüzalp[1] · Gökhan Parlakgümüş[1] · Ümmühan Özdemir Özmen[1] · Neslihan Özbek[2] · Ebru Aktan[1]

Received: 4 February 2021 / Accepted: 12 May 2021
© Iranian Chemical Society 2021

Abstract

In our present study, copper(II) sulfonamide complexes titled as bis-(2 acetylfuranmethanesulfonylhydrazone) copper(II) chloride, bis-(2-furaldehydemethanesulfonylhydrazone)copper(II) chloride and bis-(5-nitro-2 furaldehydemethanesulfonylhydrazone)copper(II) chloride were synthesized using aromatic sulfonylhydrazones derived from methane sulfonic acid hydrazide. The structures of copper(II) sulfonamides were determined by using LC–MS, FT-IR and UV–Vis methods, magnetism and conductivity measurements, and also electrochemical studies. In order to gain insight into the structure of the copper(II) complexes, computational studies were performed by using DFT/B3LYP/6-311G(*d*,*p*) basis set with the Gaussian 09 program package. In general, sulfonamides and their derivatives are researched for their inhibitory effects on carbonic anhydrase isoenzymes (CAs). Synthesized copper(II) complexes have also sulfonamide group which is the most important pharmacophore for CA inhibition efficiency like acetazolamide (AAZ) as positive control. The carbonic anhydrase I (CA I) inhibition of copper(II) complexes which goes on competitively was determined by using UV–Vis spectrophotometer technique, and their inhibition parameters such as K_m, IC_{50} and K_i were calculated. Among tested compounds, bis-(5-nitro-2 furaldehydemethanesulfonylhydrazone) copper(II) chloride was found to be the most active complex on CA I isoenzyme with IC_{50} value of 7.03×10^{-5} M. The enzyme inhibition trends of copper(II) sulfonamides on CA I isoenzyme were also investigated by CV and differential pulse voltammetry (DPV) techniques, qualitatively. The substrate of *p*-nitrophenyl acetate (PNPA) was hydrolyzed by CA I and produced *p*-nitrophenol (PNP). The electrochemical studies showed that when the concentration of the inhibitor was increased, the reduction peak current of PNP produced by the hydrolysis of PNPA was decreased by enzyme inhibition.

✉ Demet Uzun
demetuzun@gazi.edu.tr

[1] Faculty of Science, Department of Chemistry, Gazi University, 06500 Ankara, Turkey

[2] Faculty of Education, Department of Chemistry, Ahi Evran University, 40100 Kırşehir, Turkey

Published online: 25 May 2021

Graphic Abstract

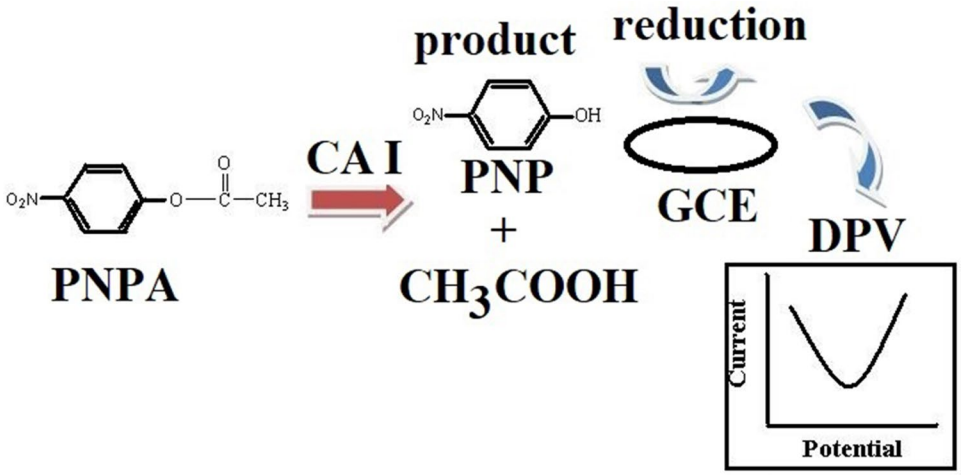

Keywords Sulfonamide · Carbonic anhydrase I · Enzyme inhibition · Voltammetry

Introduction

Carbonic anhydrase isoenzymes (CAs) containing zinc ion are widespread metalloenzymes and they classically attend in pH homeostasis maintenance [1]. CAs are very significant enzymes, which arrange CO_2 levels in living organisms. The hydration of CO_2 is catalyzed by CAs to generate bicarbonate and proton [2]. This physiological reaction acts a key role in the production of molecules, such as fatty acids, amino acids and nucleotides [3], in the ion transport mechanisms such as pH control [4]. The CA enzyme has a zinc prosthetic group coordinated in three positions by histidine side-chains. There is a special pocket for CO_2 in the active site of enzyme which brings it closer to the hydroxide group connected to the zinc. Hence, this causes the electron-rich hydroxide ion to attack CO_2 and thus form a bicarbonate molecule [5, 6]. CA structures are unique and characterized into different classes, including α-, β-, γ-, δ-, ζ-, η- and θ—anhydrases [7]. Currently, there are 16 known human CA isoforms ranging from CA I-CA XV. They differ in their cellular localization and rate of enzymatic activity [8]. CAs inhibitors are utilized in the clinical cure of various diseases such as diverse neurological disorders, acid—base disequilibria, glaucoma and gastroduodenal ulcers [1]. The syntheses and analyzes of the inhibitors of CAs from the various classes of compounds are crucial due to their specificity against isoenzymes. Sulfonamides are the best-known classes of inhibitors of CAs that are widely used in clinical medicine [9]. In this regard, a large number of aromatic/heterocyclic sulfonamides and their complexes have been prepared [10]. Recently, sulfonamides-based Schiff bases and their metal complexes were used due to their inhibitory properties toward CA I isoenzyme [11].

Electrochemical technique is the most preferred because of its simplicity, less time-consumption, high sensitivity and possibility to study without any pre-treatment with colored samples in ligand–metal interactions than many techniques [12–14]. Numerous of the significant biological processes are based on redox processes in biological systems [15].

There are some studies about investigation of the enzyme inhibition properties of some compounds by electrochemical techniques. Most of them are based on modified electrodes [16–18], biosensors [19–21]. There are only a few electrochemical studies using bare electrodes like our study. Qiu et al. developed a technique-based square wave voltammetry to evaluate impact of organophosphorus (OPs) compound on cholinesterase with a redox indicator named 2,6-dichloroindophenol (2,6-DCIP). The cholinesterase (ChE) inhibition was evaluated by measuring the enzyme activity before and after incubation with parathion-methyl [22]. Veloso et al. [23] set a droplet-based microfluidic system with electrochemical sensing in enzyme inhibition assays. Acetylcholinesterase (AChE) inhibition by Donepezil (inhibitor) using electrochemical technique was studied for Alzheimer's disease (AD). A potentiostat system was used for the determination of thiocholine (TCh) (enzymatic product) on the unmodified gold screen-printed electrode using a differential pulse voltammetry (DPV) method [24]. Some applications have been offered about metal complexes of heterocyclic sulfonamides. Especially, zinc(II) and copper(II) complexes have been studied for their strong CA inhibitory properties due to their very efficient intraocular pressure (lOP) lowering properties [25, 26]. In general, copper(II) complexes

of sulfonamides show more cytotoxic efficiency than free ligands [27].

In this study, copper(II) complexes of sulfonylhydrazones (2 acetylfuranmethanesulfonylhydrazone, 2-furaldehydemethanesulfonylhydrazone and 5-nitro-2-furaldehydemethanesulfonylhydrazone) [28] were newly synthesized and characterized by spectroscopic techniques (LC–MS, FT-IR and UV–Vis), magnetic moment, molar conductivity and redox potentials. Gaussian 09 software was used to obtain the most stable conformation of the copper(II) complexes based on DFT technique with B3LYP/6-311G(*d*,*p*) basis set. The global reactivity descriptors such as the highest occupied molecular orbital (E_{HOMO}), the lowest occupied molecular orbital (E_{LUMO}), electronegativity (χ), chemical potential (μ), global hardness (η), global softness (S), global electrophilicity index (ω) were calculated by this basis set, respectively. The CA I enzyme inhibitory effects of the copper(II) sulfonamides were determined by spectrophotometric technique. The enzyme activity of these compounds was evaluated by using K_m (Michaelis constant), IC_{50} (molarity of inhibition as 50% decrease in enzyme activity) and K_i (inhibitor–enzyme dissociation constant) values calculated by Lineweaver–Burk graph, activity% graph and Cheng–Prusoff equation. Also, the inhibitory activities of the compounds were qualitatively investigated by voltammetric techniques to support activity trend of the complexes. The enzyme activities of the copper(II) complexes were measured by the reduction of PNP (product) which produced as a result of the enzymatic hydrolysis of PNPA by CA I. In the presence of inhibitor, the peak current of PNP was decreased as a result of inhibition of enzyme function. The copper(II) complexes acted as stronger inhibitors of CA I meanwhile compared to uncomplexed sulfonamides [28] from which they were derived. The inhibition studies show that NO_2 substituted compounds have higher enzyme inhibition activities than others.

Experimental

Chemicals, reagents and instrumentation

The reagents commercially available used in the studies were of the analytical grade. CA I isoenzyme having high purity was purchased from Sigma-Aldrich. AAZ was also purchased from Sigma-Aldrich. Acetonitrile (ACN), tetrabutylammonium tetrafluoroborate (TBATFB), TRIS and H_2SO_4 were purchased from Merck. Ultrapure quality of water (18.3 MΩ) (Millipore Corp. Bedford, MA (USA)) was used to prepare aqueous solutions and clean to polished electrodes.

The infrared (IR) spectra were recorded in the range of 4000–400 cm^{-1} for sulfonamide compounds as KBr-disks with a Mattson-1000 FT-IR spectrometer. UNICAM-UV 2–100 spectrophotometer was used for UV–Vis spectra measurements. A Gallenkamp melting point apparatus was used to determine melting points of compounds.

Electrochemical experiments of differential pulse voltammograms (DPVs) and cyclic voltammograms (CVs) were conducted on a CH Instrument 660B electrochemical workstation. As working electrode with a 3 mm diameter, a glassy carbon (GC) electrode was used. As reference electrodes, a Ag/AgCl electrode in aqueous medium and a Ag/Ag^+ (0.01 M) electrode in nonaqueous medium were used. A platinum wire was a counter electrode in conventional three-electrode system. Herein, nonaqueous medium is an ACN solution that contains 0.1 M TBATFB. As supporting electrolyte solution, TRIS buffer at pH 7.4 with a 10 mM concentration prepared using 1 M H_2SO_4 was used in the enzyme inhibition studies. Stock solutions of compounds called inhibitors (1 mM) were prepared at room temperature in nonaqueous medium.

To polish GC electrode, alumina slurry (0.05 µm) was used. After polishing electrode, it was sonicated for 10 min in ultrapure water and then with a mixture of isopropyl alcohol/ACN (1:1 (v/v)). To dry it N_2 (99.999%) stream was used.

Computational studies

All quantum chemical calculations for copper(II) complexes were performed by Gaussian 09 quantum chemistry program package examined with Becke's three-parameter exchange functional in combination with the Lee–Yang–Parr correlation functional (B3LYP) in density functional theory (DFT) method with 6-311G(*d*,*p*) basis set. The highest occupied molecular orbital (HOMO) and the lowest unoccupied molecular orbital (LUMO) known as FMOs are very important for quantum chemistry [29]. The HOMO and LUMO energies are directly related to the ionization potential and electron affinity. The global reactivity descriptors such as ionization potential ($I = -E_{HOMO}$), electron affinity ($A = -E_{LUMO}$), energy band gap ($\Delta E = E_{LUMO} - E_{HOMO}$), electronegativity ($\chi = (I + A)/2$), chemical potential ($\mu = -\chi$), global hardness ($\eta = (I - A)/2$), global softness ($S = 1/2\eta$) and global electrophilicity index ($\omega = \mu^2/2\eta$) were used to predict global reactivity trends relating with structural properties [29].

General procedure for the synthesis of copper(II) complexes

A methanolic solution of copper(II) chloride was added dropwise to the methanolic solution of sulfonylhydrazone ligands by the molar ratio of 1:2 by stirring at 40 °C. Then, the reaction mixture was refluxed for 2 days at 40 °C and

Scheme 1 The structures of CA I inhibitors

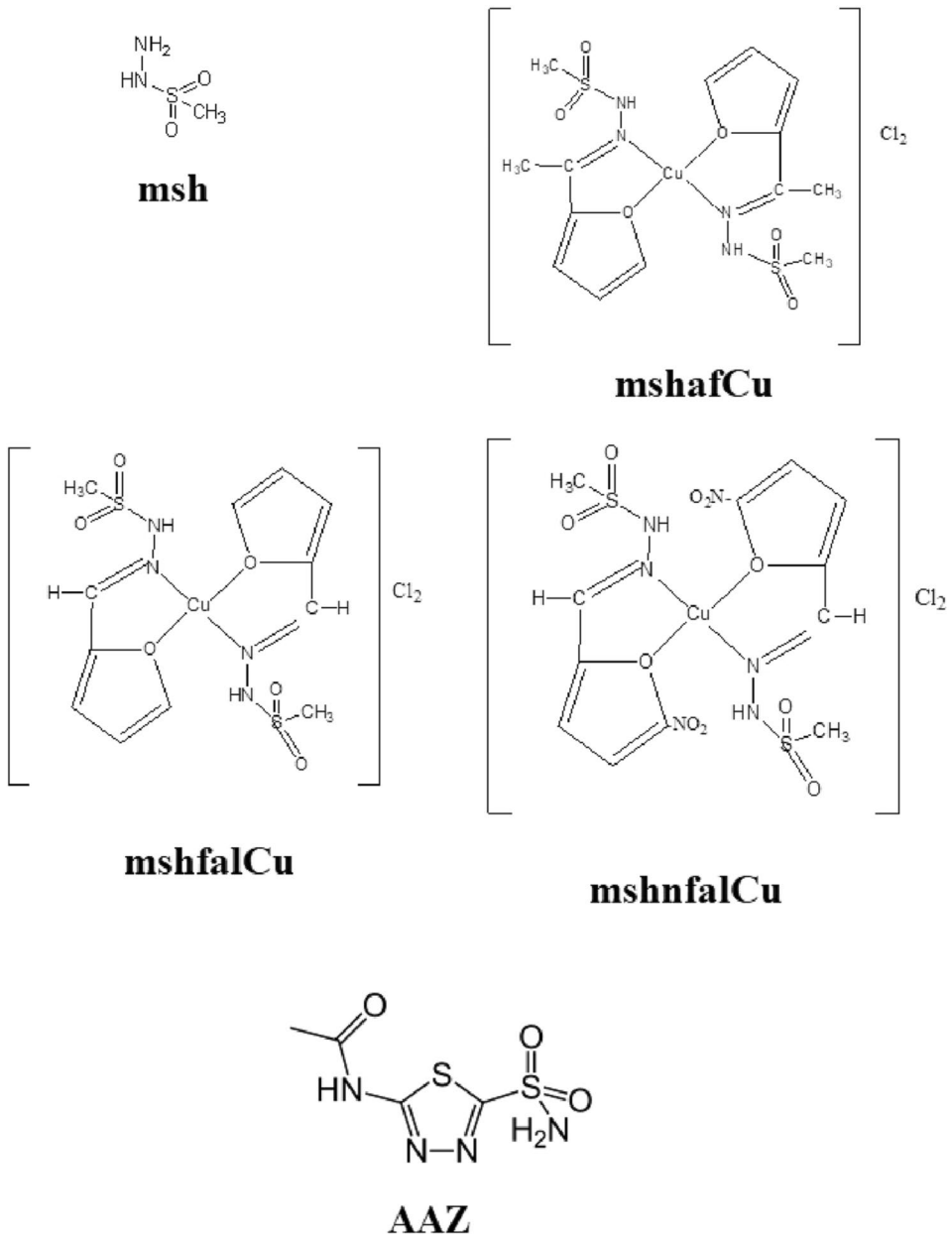

then concentrated to half of volume. The resulting product was allowed to stand for 1–2 weeks in the room temperature and obtained crystals were recrystallized from methanol/ethylacetate, washed by ether solvents and purified crystals were dried in oven at 50 °C.

Spectral data for copper(II) complexes

Bis-(2-acetylfuranmethanesulfonylhydrazone) copper(II) chloride [Cu(mshaf)$_2$]Cl$_2$ (mshafCu) ($C_{14}H_{20}N_4O_6S_2Cl_2Cu$, MW = 538.91 g/mol): Yield % = 51; mp = > 200 °C; μ_{eff} = 2.22 BM; λ_{max} = 370 nm, 245 nm; $\wedge_M$ = 152.4 $\Omega^{-1}.cm^2.mol^{-1}$ (1:2 electrolyte); IR(cm^{-1}): $\upsilon(NH_2)$ 3242, $\nu_{(C=N)}$ 1619, $\nu(SO_2)$ 1331, $\nu_{(C–O–C)}$ 1258, δ(NH) 636, $\delta(SO_2)$ 534; LC–MS ~ m/z(%): 267(100), 539(2).

Bis-(2-furaldehydemethanesulfonylhydrazone) copper(II) chloride [Cu(mshfal)$_2$]Cl$_2$ (mshfalCu) ($C_{12}H_{16}N_4O_6S_2Cl_2Cu$, MW = 510.85 g/mol): Yield % = 56; mp = 130 °C; μ_{eff} = 2.28 BM; λ_{max} = 370 nm, 245 nm; $\wedge_M$ = 122.3 Ω^{-1} cm^2 mol^{-1} (1:2 electrolyte), IR(cm^{-1}): $\upsilon(NH_2)$ 3238, $\nu_{(C=N)}$ 1619, $\nu(SO_2)$ 1339-1303, $\nu_{(C–O–C)}$ 1206, δ(NH) 617, $\delta(SO_2)$ 532; LC–MS ~ m/z(%): 391(100), 454(12).

Bis-(5-nitro-2-furaldehydemethanesulfonylhydrazone) copper(II) chloride [Cu(mshnfal)$_2$]Cl$_2$ (mshnfalCu)

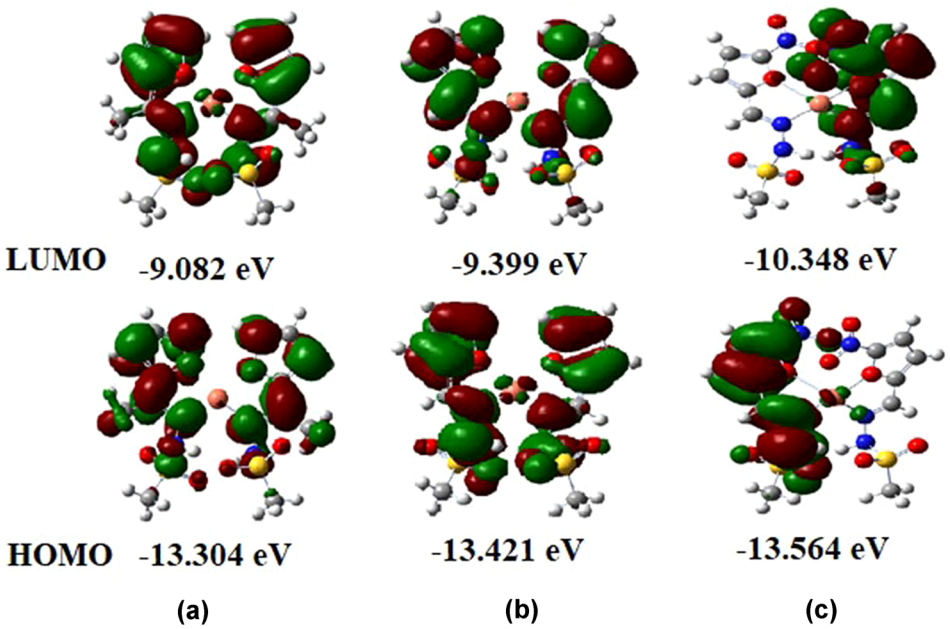

Fig. 1 FMOs (HOMO and LUMO) of copper(II) complexes; **a** mshafCu, **b** mshfalCu and **c** mshnfalCu

Table 1 Calculated FMOs (HOMO and LUMO) energies and global reactivity descriptors

Compound	E_{HOMON} (eV)	E_{LUMO} (eV)	ΔE (eV)	χ (eV)	μ (eV)	η (eV)	S $(eV)^{-1}$	ω (eV)
mshafCu	− 13.304	− 9.082	4.222	11.193	− 11.193	2.111	0.237	29.675
mshfalCu	− 13.421	− 9.399	4.022	11.410	− 11.410	2.011	0.249	32.367
mshnfalCu	− 13.564	− 10.348	3.216	11.956	− 11.956	1.608	0.311	44.456

($C_{12}H_{14}N_6O_{10}S_2Cl_2Cu$, MW = 600.85 g/mol): Yield % = 48; mp = 160 °C; μ_{eff} = 2.27 BM; λ_{max} = 390 nm, 240 nm; $\wedge_M$ = 143.5 Ω^{-1} cm^2 mol^{-1} (1:2 electrolyte); IR(cm^{-1}): $\upsilon(NH_2)$ 3239, $\nu_{(C=N)}$ 1634-1619, $\nu(SO_2)$ 1356, $\nu_{(C–O–C)}$ 1201, δ(NH) 622, $\delta(SO_2)$ 566; LC–MS ~ m/z(%): 465(100), 610(7).

Results and discussion

Characterization studies of copper(II) complexes

The copper(II) sulfonamides (Scheme 1) were synthesized using sulfonylhydrazones derived from methane sulfonic acid hydrazide (msh) and characterized by spectroscopic (LC–MS, FT-IR and UV–Vis), magnetism, conductivity and electrochemical studies. The geometry optimization and electronic parameters of copper(II) complexes were performed on DFT/B3LYP/6-311G(*d*,*p*) methods with Gaussian 09 program. The CA I inhibition activities of copper(II) complexes and AAZ standard were investigated by spectroscopic technique. The K_m, IC_{50} and K_i parameters relating with inhibition effect were determined, respectively. Also, electrochemical behaviors of the compounds were studied during the inhibitor–enzyme interaction, qualitatively.

LC/MS spectra

LC/MS shows that molecular ion and basic peaks for complexes; mshafCu, mshfalCu and mshnafCu are exhibited at m/z(%); 267(100) and 539(2), 391(100) and 454(12), 465(100) and 610(7), respectively.

FT-IR spectra

The selected IR vibration frequencies of copper(II) complexes are presented in experimental part. The assignment of the bands is made by taking into consideration the literature data for compounds containing appropriate structural fragments such as imine (C=N) and sulfonamide ($NH–SO_2$) groups [28, 29]. The imine (C=N) group was obtained by the condensation of primer amines with aldehydes or ketones. The imine stretchings ν(C=N) of mshafCu, mshfalCu and mshnfalCu were observed at 1619 cm^{-1}, 1619 cm^{-1} and 1634–1619 cm^{-1} as strong band. The vibrations belonging to sulfonamide group were observed between 3242 and 3238 cm^{-1} for υ(NH), 1356–1303 cm^{-1} for $\upsilon(SO_2)$, 636–617 cm^{-1} for δ(NH) and 566–532 cm^{-1} for $\delta(SO_2)$, respectively.

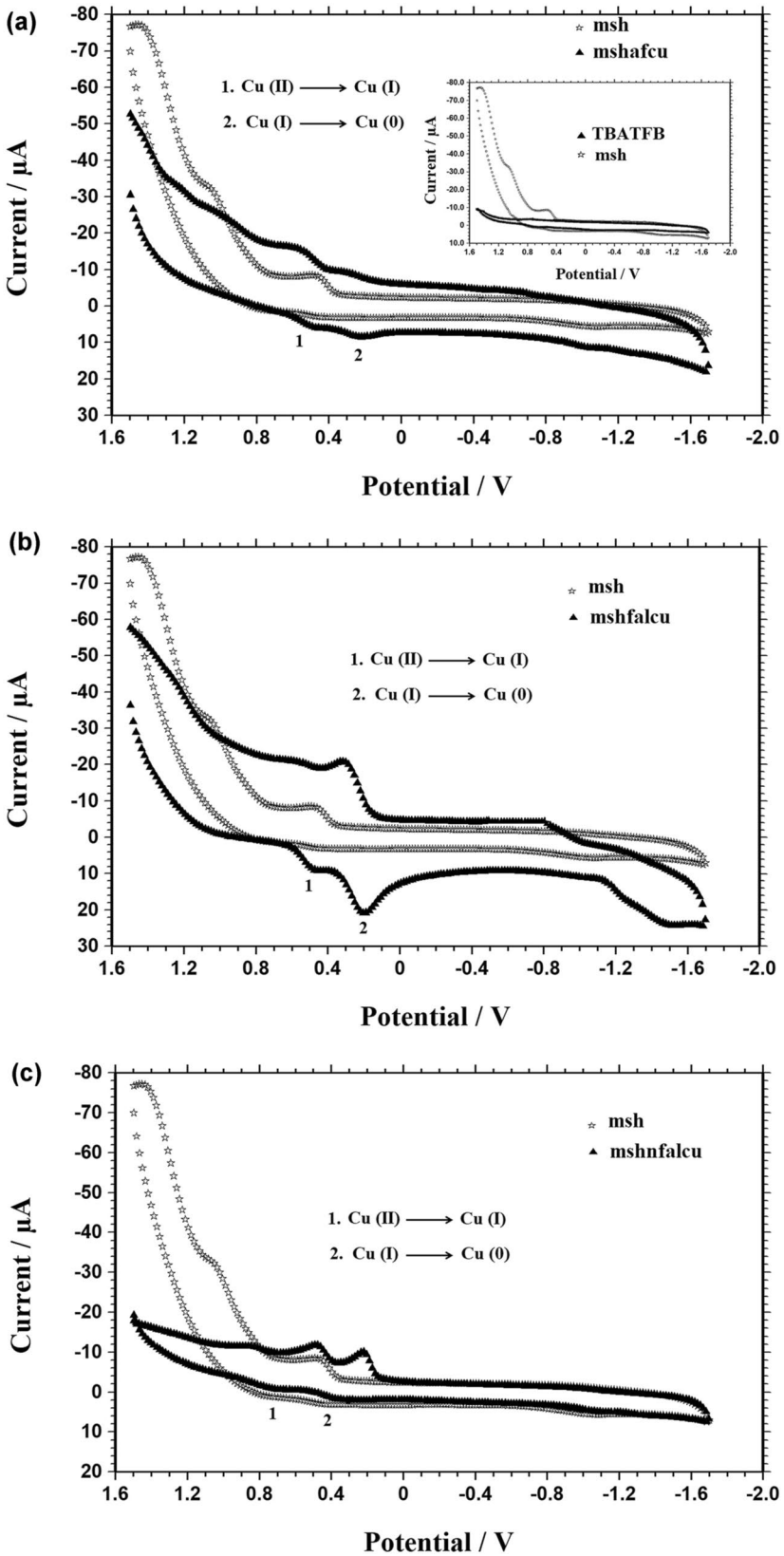

Fig. 2 The CVs of 1 mM **a** msh and mshafCu, **b** msh and mshfalCu and **c** msh and mshnfalCu on the GC electrode in ACN containing 0.1 M TBATFB as supporting electrolyte. The CVs belonging to msh and supporting electrolyte are at the top on the right-hand side of Fig. 2a

The frontier molecular orbitals (FMOs) and global reactivity descriptors

The FMOs distribution and energy levels for the complexes were computed on optimized geometries by using B3LYP/6-311G (*d*,*p*) basis set and HOMO–LUMO shapes are presented in Fig. 1. The FMOs (HOMO and LUMO) are the main orbitals taking part in chemical reaction. Conventionally, the singly occupied molecular orbital (SOMO) is also considered to be the highest occupied molecular orbital (HOMO) as presented in this report for copper(II) complexes having d^9 electronic configuration system with one unpaired electron.

The global reactivity descriptors containing electronegativity (χ), chemical potential (μ), global hardness (η), global softness (s) and global electrophilicity index (ω) were calculated by FMOs energies (E_{HOMO} and E_{LUMO}) and are listed in Table 1. In all complexes, mshnfalCu with NO_2 group has the lowest LUMO energy (− 10.348 eV) and gap (3.216 eV) levels that are the most important descriptors showing the tendency of any species to accept electrons. The highest electrophilicity ($\omega = 44.456$ eV) of mshnfalCu may be concluded as good global chemical reactivity for drug metabolism [29].

Electrochemical behaviors of copper(II) complexes

The electrochemical behaviors of the sulfonamides and their derivatives may be helpful for widespread usage in the drug industry [30]. Many biological processes (bio-reduction/bio-oxidation) are based on redox reactions. So, there is a correlation between electrochemistry and biological activity.

Redox properties of copper(II) sulfonamides were investigated by cyclic voltammetry (CV) technique. The CVs of copper(II) complexes were recorded in ACN containing 0.1 M TBATFB (supporting electrolyte) under N_2 stream between − 1.7 and 1.5 V with a sweep rate of 0.1 V s^{-1} as exhibited in Fig. 2. The CVs belonging to copper(II) complexes of sulfonamides were compared with that of the amine named methane sulfonic acid hydrazide (msh) mentioned in our first study [28].

In the positive range, two oxidation peaks due to sulfonamide group were observed in the voltammogram of the complexes [31, 32]. To observe the changes, copper(II) complexes were compared with sulfonamide (msh). The copper(II) complexes showed reduction peaks belong to Cu at about the potential 0.452 V; 0.483 V and 0.673 V for mshafCu, mshfalCu and mshnfalCu, respectively. This can be assigned as Cu(II)/Cu(I) reduction process. In addition, Cu(I)/Cu (0) reduction process was viewed at 0.215 V; 0.199 V and 0.325 V for these complexes, respectively [33].

A shift of the oxidation or reduction potentials was caused by electron donating or withdrawing effects of substituents. When looking at the copper(II) complexes of the ligands (the ligands were given in our previous study), the reduction peaks belonging to the imine (–C=N–) group could not be observed due to the complexation between the nitrogen atoms and oxygen (in the furan ring) with metal ions so has no trendy with activity. The potentials of the anodic peaks were shifted to more positive potentials with the increasing scan rate as expected for an irreversible process [34]. The irreversibility of the redox processes in the complexes was attributed to the changes in the coordination geometry or coordination number upon change of the oxidation state [35]. Tetrahedral geometry of copper(II) complex may be the reason of the having higher activity [35]. Electron donating substituents $–CH_3$ caused a peak shift to more positive potentials, while on the other side electron withdrawing substituents $–NO_2$ caused a peak shift toward lower potentials, facilitating the oxidation [36]. The decreasing oxidation potential of mshnfalCu that contains NO_2 group may be explained by the increasing activity of this compound [36, 37].

The influence of sweep rate on the oxidation of inhibitors

The influences of sweep rates (ν) on the first oxidation peak currents of 1 mM inhibitors on the GC surface were examined in the range from 0.01 to 0.5 V s^{-1} between − 1 V and 1.5 V. The slopes of log ip versus log v, which are equal to approximately 0.5 for all of the inhibitors (Fig. 3), indicate that the electrode process on the GC electrode surface in nonaqueous medium was controlled by diffusion [38].

Determination of inhibition effects of copper(II) complexes on CA I

Enzyme inhibition studies by spectrophotometric technique

The activities of CA were assayed by the hydrolysis of substrate PNPA [39] to PNP via CA I isoenzyme. The enzyme activities of the inhibitors (mshafCu, msfalCu, mshnfalCu and AAZ as standard) were firstly evaluated by the spectrophotometric technique. The activity parameters of K_m (Michaelis constant), IC_{50} (molarity of inhibition as 50% decrease in enzyme activity) and K_i (inhibitor–enzyme dissociation constant) were calculated with Lineweaver–Burk graph, activity%—[inhibitor] graph (Fig. 4) and Cheng–Prusoff equation, respectively [40, 41]. IC_{50} and K_i values are the most suitable parameters that show the inhibitory effect of an inhibitor. 3.0 mM PNPA and four different concentrations (1×10^{-2}, 1×10^{-3}, 1×10^{-4}, 1×10^{-5} M) of inhibitors were used to determine IC_{50} values. Reaction was started by adding of 0.05 M tris-SO_4 buffer (pH: 7.4) and 0.1 mL

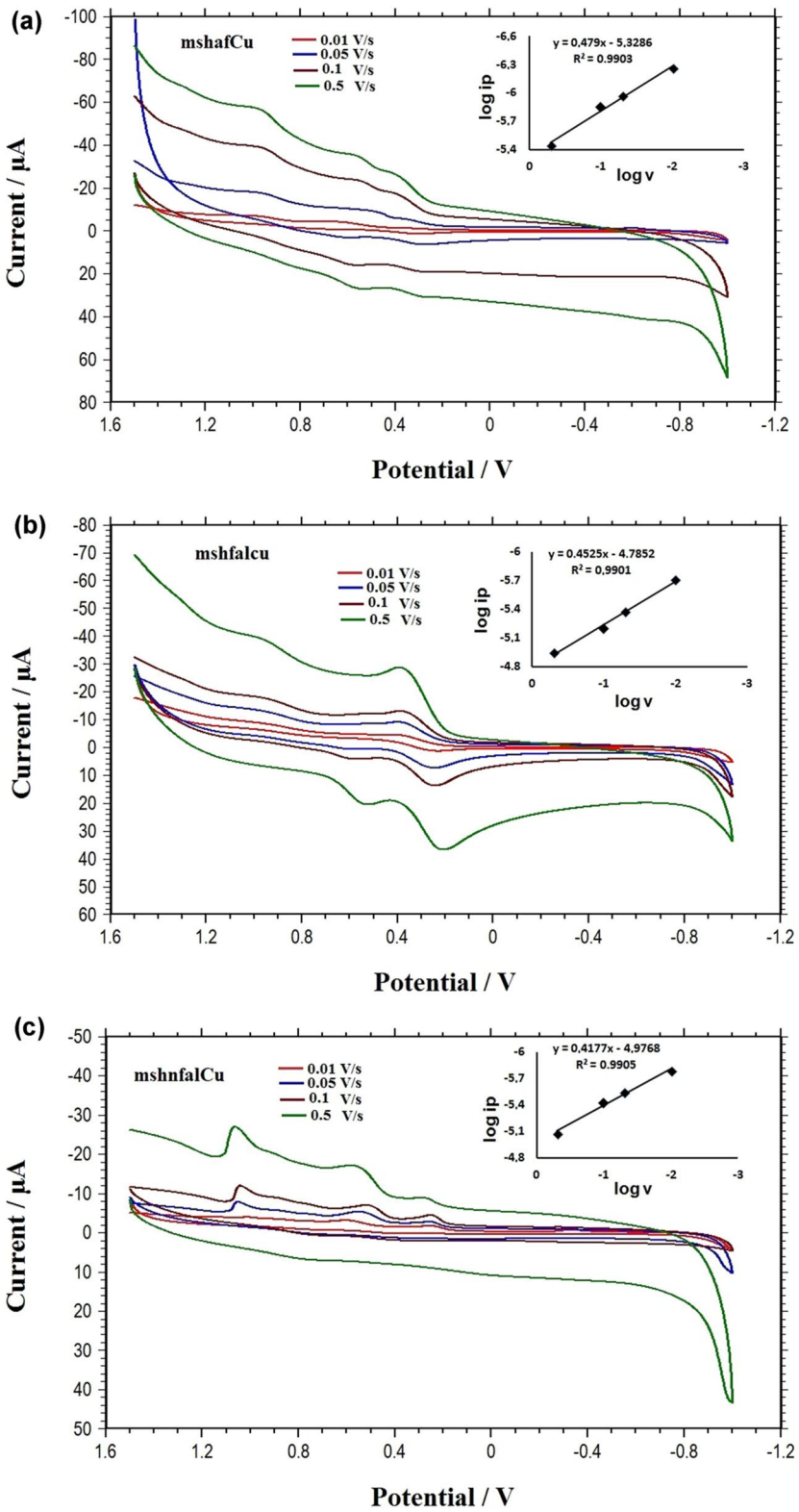

Fig. 3 The CVs and log ip-log *v* graphs of 1 mM **a** mshafCu, **b** msfalCu and **c** mshnfalCu at different sweep rates (0.01; 0.05; 0.1 and 0.5 V/s) (vs. Ag/Ag^+) in ACN containing 0.1 M TBATFB

enzyme solution. The absorbance of the product (PNP) was determined at 400 nm after 6 min [6, 42]. This study was repeated three times for each inhibitor. The concentrations of substrate were taken 0.3, 0.6, 1.0, 3.0 mM without or with inhibitor in the medium. The K_m values were found by drawing the Lineweaver–Burk graph (Fig. 4) and then K_i values were calculated based on K_m and IC_{50} values. Figure 4 is given for only 1 inhibitor (mshnfalCu). The values of

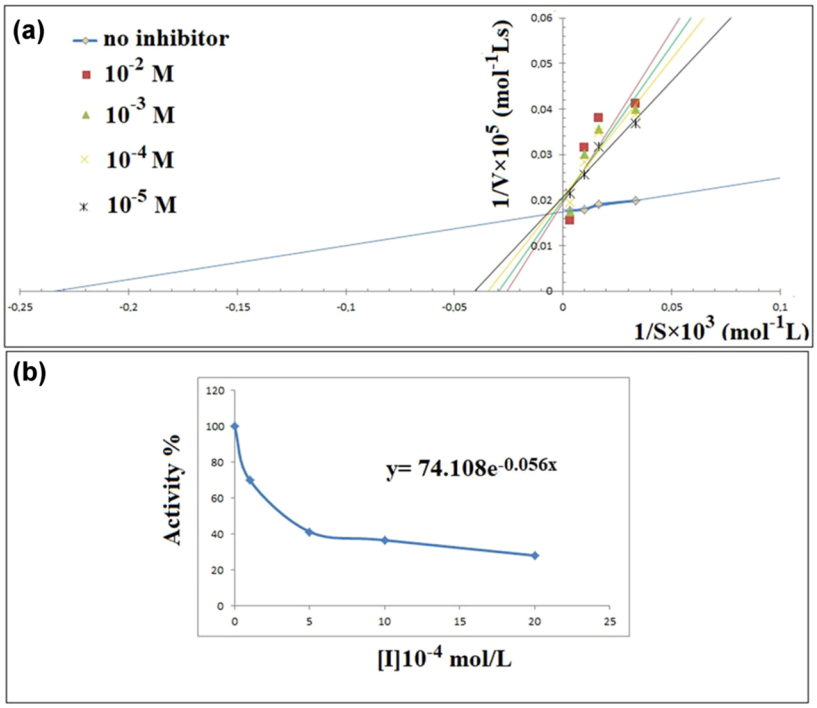

Fig. 4 The graphs of **a** Lineweaver–Burk and **b** Activity % belong to mshnfalCu

Table 2 The results of enzyme inhibition activities of copper(II) complexes and AAZ

Compound (Inhibitor)	K_m (M)	IC_{50} (M)	Average K_i (M)	Inhibition type
mshafCu	34.80×10^{-5} 30.70×10^{-5} 28.30×10^{-5} 22.30×10^{-5}	7.91×10^{-5}	3.75×10^{-6}	Competitive
mshfalCu	36.57×10^{-5} 32.11×10^{-5} 27.61×10^{-5} 22.30×10^{-5}	7.30×10^{-5}	2.30×10^{-6}	Competitive
mshnfalCu	38.40×10^{-5} 33.70×10^{-5} 28.90×10^{-5} 24.40×10^{-5}	7.03×10^{-5}	1.45×10^{-6}	Competitive
AAZ	64.94×10^{-5} 55.96×10^{-5} 46.97×10^{-5} 39.64×10^{-5}	5.47×10^{-5}	7.03×10^{-6}	Competitive

activity parameters for all copper(II) complexes and positive control AAZ are given in Table 2 [43]. The kinetics parameters (IC_{50} and K_i) of the sulfonylhydrazone ligands previously reported by our groups were calculated using activity%—[inhibitor] graph and Cheng–Prusoff equation. The K_i and IC_{50} values of the ligands were found 2.55×10^{-5} M and 1.12×10^{-3} M for mshaf, 1.28×10^{-5} M and 1.10×10^{-3} M for mshfal and 5.88×10^{-6} M and 1.02×10^{-4} M for mshnfal, respectively [28]. As seen in Table 2, copper(II) complexes behaved as good inhibitors against CA I isoenzyme compared with their free ligands. The mshnfalCu complex having the lowest IC_{50} (7.03×10^{-5} M) showed the highest inhibition effect on CA I than other copper(II) complexes, because it contains highly electron withdrawing group (NO_2) which may play an important role in biological activities. When the inhibition activity parameters of the copper(II) complexes were compared with AAZ used as an inhibitor drug in glaucoma treatment, they are found to have good inhibition effects.

The enzyme inhibitors can inhibit the enzyme catalytic activity either irreversibly or reversibly. In reversible inhibition, the inhibitors bind non-covalently to the active

Scheme 2 The forms of reversible enzyme inhibition

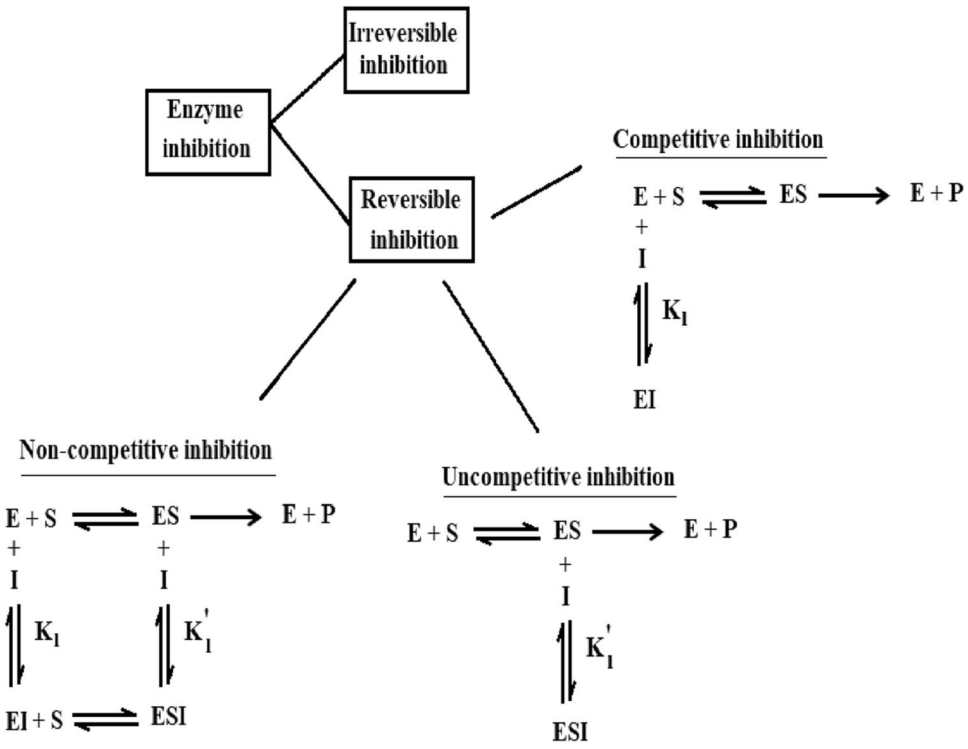

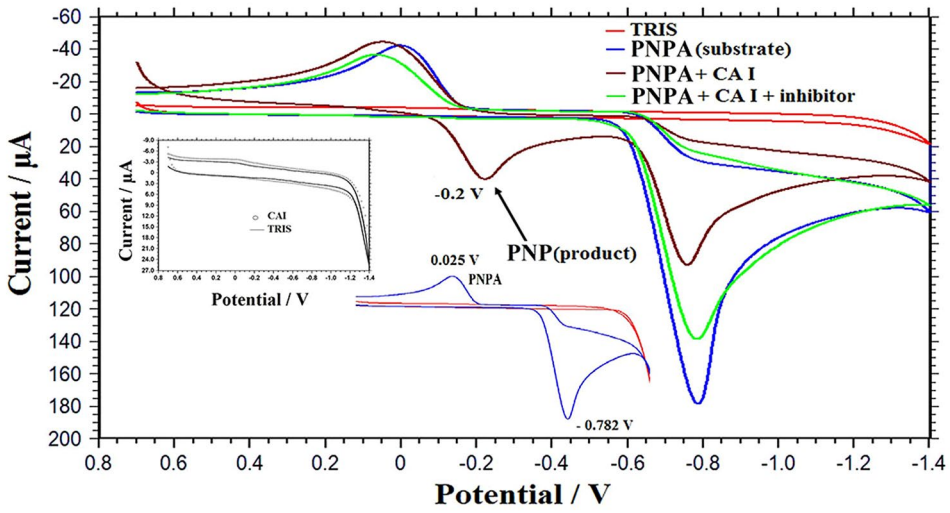

Fig. 5 The CVs on the GC electrode for CA I samples that contain 5 µL CA I, 3 mM PNPA and 1×10^{-4} M inhibitor in the cell. The PNP cathodic peak potential (− 0.2 V) was compared with PNPA (− 0.782 V; 0.025 V). The medium is pH 7.4 TRIS buffer with 10 mM concentration (vs. Ag/AgCl)

site of the enzymes and can be easily removed from the enzyme–inhibitor complex. The competitive inhibitors (I) compete with the substrate (*S*) to interact with the active site of the enzyme (*E*) and thus prevents binding of the substrate as in this study. The uncompetitive inhibitors bind to the enzyme–substrate complex (ES) or enzyme forms. Also, the noncompetitive inhibitors bind either the enzyme (*E*) and enzyme–substrate complex (ES*)* or enzyme forms [44, 45]. The forms of reversible enzyme inhibition [44] were given in Scheme 2.

All copper(II) sulfonamide complexes showed competitive inhibition, reversibly (Table 2).

Enzyme inhibition studies by electrochemical technique

The CA I inhibition activities of copper(II) complexes were also studied qualitatively by electrochemical technique. For this purpose, the CVs at a sweep rate of 100 mV s^{-1} were taken in pH 7.4 TRIS buffer medium containing 3 mM PNPA and then CA I (5 µL) enzyme in the cell. The potential of CVs was applied between − 1.4 V and 0.70 V.

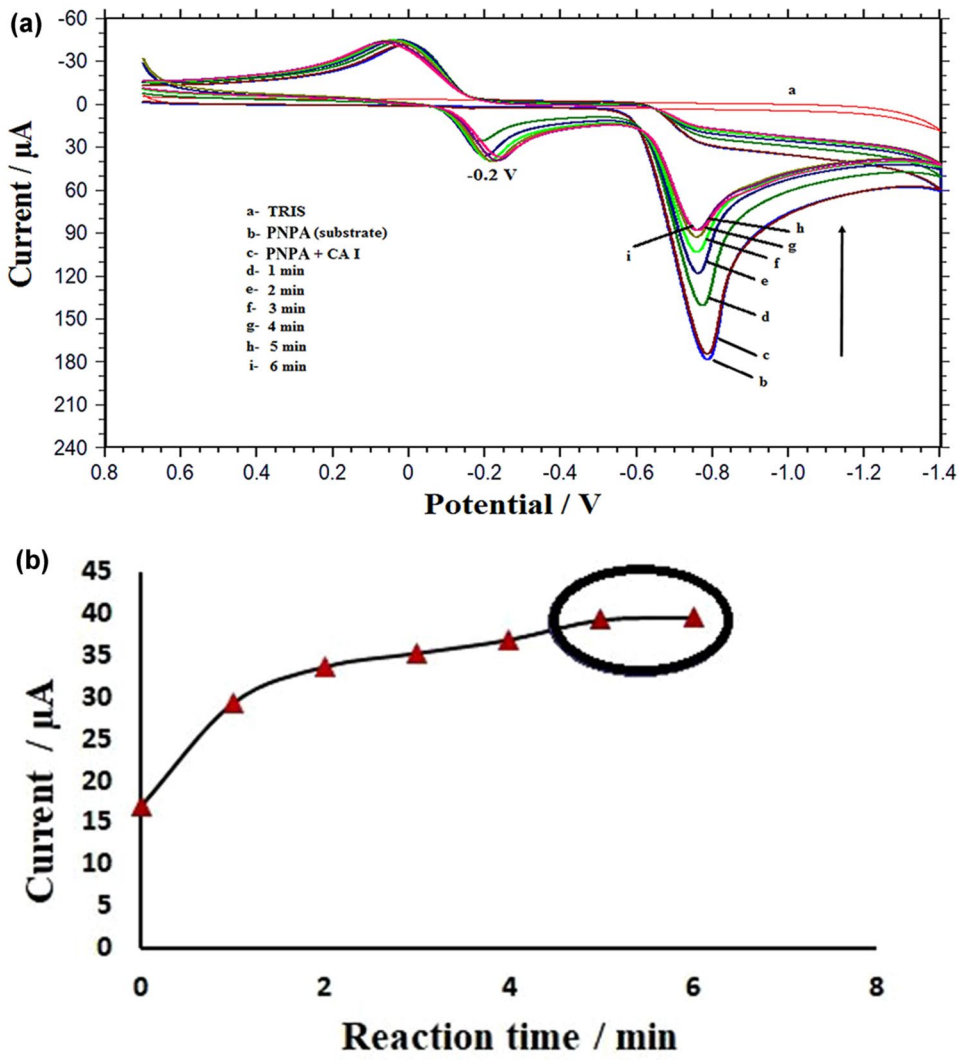

Fig. 6 **a** The CVs obtained on the GC electrode after 1, 2, 3, 4, 5 and 6 min of the enzyme reaction between 5 µL CA I and PNPA (3 mM) in pH 7.4 TRIS buffer at a sweep rate 100 mV s^{-1}. **b** The time dependence graph of the PNP reduction current with CA I catalytic reaction

In Fig. 5, it was seen that the activity of CA I is related to the decrease in the substrate PNPA and the increase in the product PNP. In the absence of TRIS and enzyme, the electrode had no response (Fig. 5) while PNPA exhibited a reduction and an oxidation peak at about − 0.782 V and 0.025 V, respectively. Clearly, PNP, was produced from the reaction between PNPA and CA I in the aqueous solution. It has a single cathodic peak versus Ag/AgCl at about − 0.2 V. It is reduced to 4-hydroxylaminophenol according to the literature report [46].

The function of the enzyme was inhibited by inhibitors; therefore, PNP formation was decreased as shown in Fig. 5 (for only 1 inhibitor was given). Thus, the CA I inhibition degree is associated with the decrease in the reduction current of PNP which depends on inhibitor concentration in the sample.

When the CA I enzyme was added into electrochemical cell, the substrate (PNPA) has two peaks while product (PNP) has one peak occurred at about − 0.2 V. Although the intensity of PNPA was higher than PNP, it was preferred to follow PNP peaks in the CV voltammograms. Both PNPA peaks could be affected differently with the addition of the inhibitors. Because, the inhibitors have some reduction and oxidation peaks that can be overlap with the PNPA peaks and it could be difficult following these peaks due to interfering effects of the inhibitors. There are no peaks at about − 0.2 V so, the reduction peak of PNP was not affected by inhibitors.

The influence of the time on PNPA hydrolysis

The influence of the time variation on the PNPA hydrolysis by CA I was studied in pH 7.4 TRIS buffer in Fig. 6a. The time versus hydrolysis of substrate (Fig. 6b) showed a gradual increase in the current of product (PNP) and a decrease in the current of substrate (PNPA) from 1 to 6 min and a

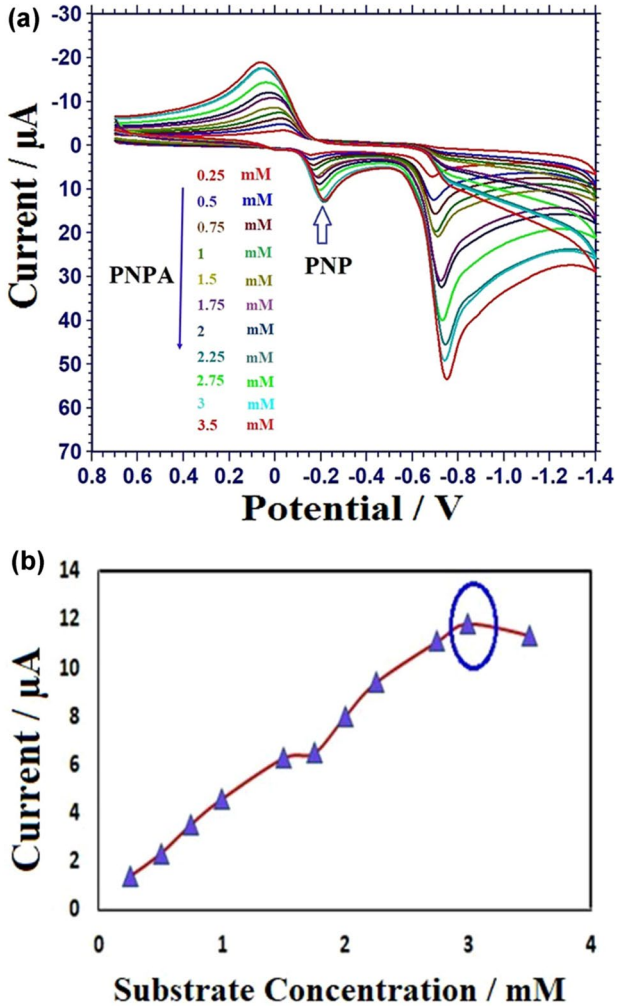

Fig. 7 **a** The CVs of the GC electrode in TRIS buffer after the enzymatic reaction with different concentrations of PNPA with 5 µL CA I. Sweep rate: 100 mV s^{-1}. **b** Electrochemical signal of PNP as a function of the concentration of substrate

plateau level reached at 6 min. Because whole enzymatic reaction was supposed to complete in this range, electrochemical scanning time was selected as 6 min.

The influence of the concentration of substrate on enzyme catalysis

The influence of substrate concentration on PNP formation was studied by CV technique. To choose an appropriate substrate concentration for the enzyme inhibition studies is very important. The substrate concentration was selected in the range of 0.25 mM–3.5 mM (Fig. 7a). The PNP formation was increased until 3 mM and then its current was decreased (Fig. 7b); in this case, 3 mM was taken as an optimum concentration of substrate.

The influences of inhibitor concentration on CA I enzyme

The effects of inhibitor concentration between 0.1 and 50 µM on the peak of the product were investigated by the DPV technique. The product was formed after the enzyme interaction with the substrate.

From the DPV voltammograms obtained by negative sweep, the reduction peak belonging to PNP is observed in Fig. 8. When CA I enzyme was inhibited by copper(II) sulfonamides, PNP formation was decreased as known. In this medium, sulfonamide anions were formed and probably bind to Zn(II) ion within enzyme active site, while the metal ions block the proton shuttle residues of CA I [26]. Therefore, the decrease rate of the reduction peak of PNP was utilized to evaluate the CA I activities of the inhibitors.

Between 0.10 V and − 0.50 V, the applied potential window, sulfonamides exhibited no detectable cathodic peaks. Nevertheless, a distinct drop in the peak current intensity was observed at about − 0.2 V suggesting that the production of PNP was inhibited, consistent with Fig. 8. According to this, the analysis on a wider sulfonamides concentrations range that is from 0.1 to 50 µM showed a gradual decrease in the peak current intensity of PNP as inhibitor concentration was increased which revealed inhibition of the CA I activity [23]. At complete inhibition (in the presence of 50 µM inhibitors), the peak current at about − 0.2 V saturated to a minimum current value measured in the absence of PNPA substrate.

To better scrutinize the inhibitory effects of the complexes, 0.5 µM was chosen as the inhibitor concentration at which the enzyme was inhibited and is given in the DPV plot in Fig. 9.

The CA I inhibition activities of the compounds decrease in following order: mshnfalCu > mshfalCu > mshafCu > msh. Also, compared with AAZ (the standard substance), the inhibitory properties of copper(II) complexes especially mshnfalcu are found to be good.

Conclusions

In this study, the synthesis of copper(II) complexes of sulfonylhydrazones derived from methanesulfonicacidehydrazide (msh) was reported. The structural characterization of mshafCu, mshfalCu and mshnfalCu complexes was made by using spectroscopic and electrochemical techniques. Based on physicochemical evidence, the proposed structure of copper(II) complexes was exhibited. The enzyme inhibition effects of the complexes were evaluated using activity parameters (K_m, IC_{50} and K_i) found by spectrophotometric technique. The highest K_i and the lowest IC_{50} values are responsible from the strongest CA I inhibition activities. mshnfalCu (the lowest IC_{50}, 7.03×10^{-5} M)

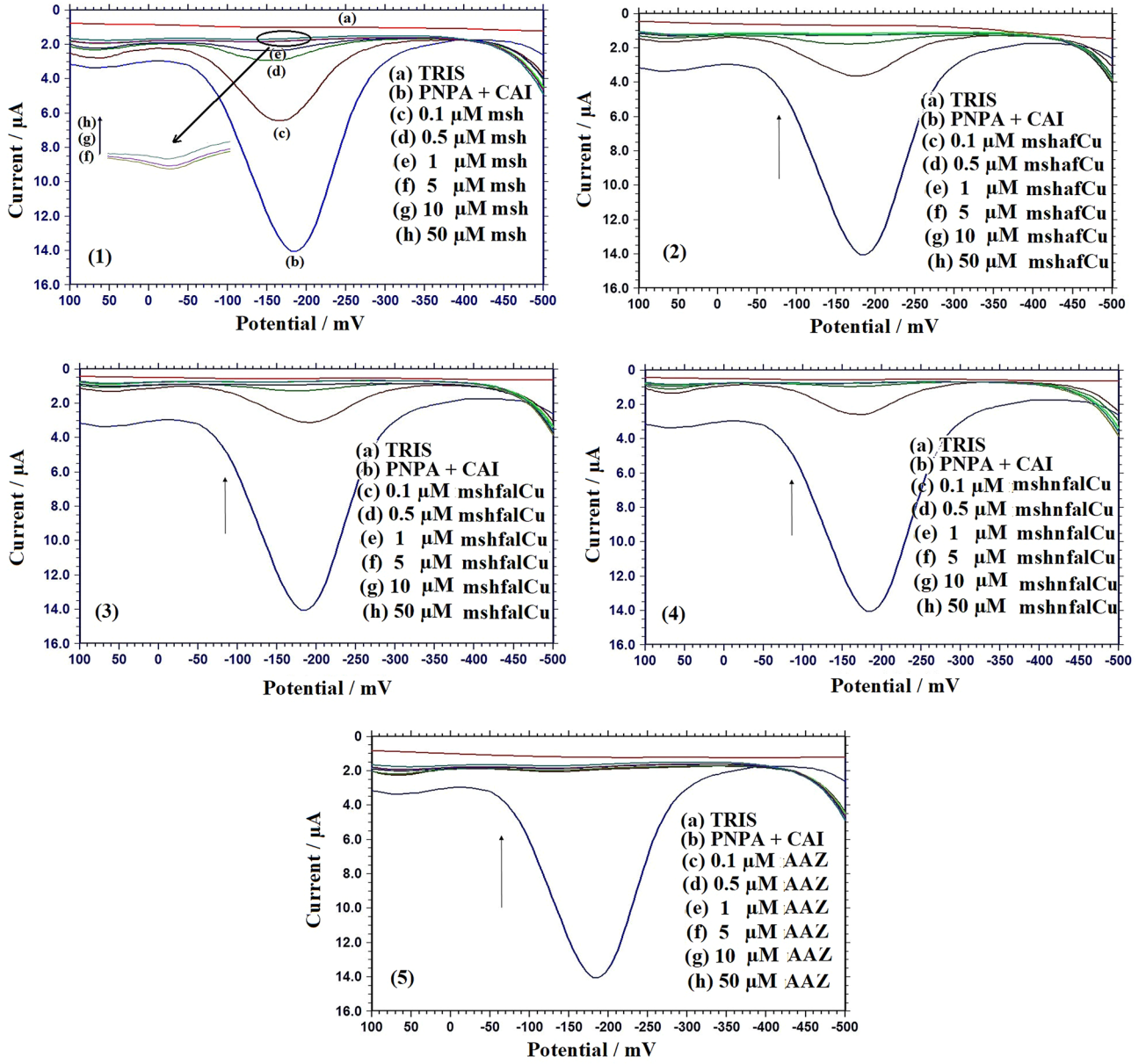

Fig. 8 The DPVs on the GC belong to PNP reduction in the presence of (1) msh, (2) mshafCu, (3) mshfalCu, (4) mshnfalCu and (5) AAZ with different concentrations. The potential was applied between 100 mV and − 500 mV versus Ag/AgCl in 10 mM TRIS containing 3 mM PNPA, 5 µL CAI and increasing concentrations of inhibitors (0.1–50 µM) at pH 7.4

has remarkable inhibition activities which may be arising from electron withdrawing group (NO_2). The quantum chemical approaches may also contribute to brighten the structure–activity relationship of the target compounds. In the electrochemical studies, CVs of the copper(II) complexes showed similar redox behaviors of free ligand. The hydrolysis reaction between CA I and substrate (PNPA) to produce product (PNP) was observed on CV voltammogram. When the inhibitor was added into electrocell, the conversion of PNPA to PNP was decreased by CA I inhibition. Electrochemical scans showed that mshnfalCu complex behaved as the strongest CA I inhibitor in others. Due to the similar trend in enzyme inhibition activities obtained by

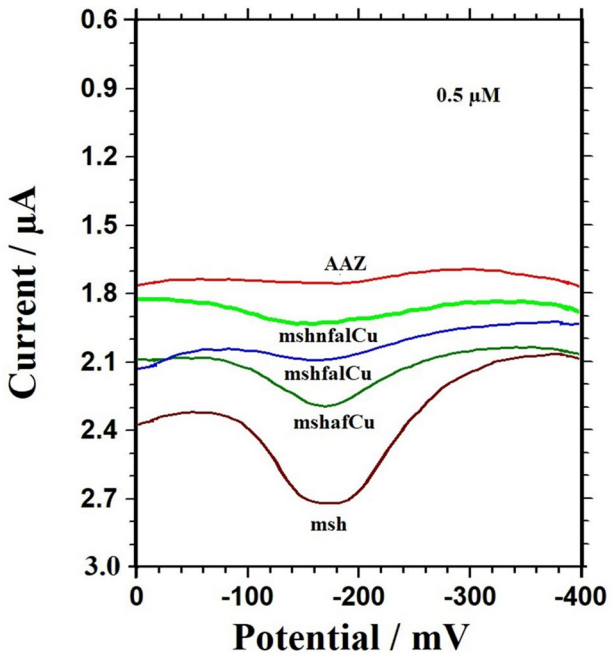

Fig. 9 Comparison of the peak currents of msh, mshafCu, mshfalCu, mshnfalCu and AAZ by DPV technique (inhibitors are at the same concentration (0.5 µM))

comparative studies, the electrochemical scanning may be an alternative technique for simple and efficient detection of CA I inhibition.

Acknowledgements This research was funded by Gazi University Research Found under Project No. 05/2011-27.

Declarations

Conflicts of interest The authors proclaimed that they have no conflicts of interest. The authors alone are responsible for the content and writing of the paper.

References

1. F. Saczewski, A. Innocenti, Z. Brzozowski, J. Sławin 'Ski, E.B. Pomarnacka, A. Kornicka, A. Scozzafava, C.T. Supuran, J. Enzyme Inhib. Med. Chem. **21**, 563–568 (2006)
2. C.T. Supuran, A. Scozzafava, Bioorg. Med. Chem. **15**, 4336–4350 (2007)
3. A. Angeli, M. Pinteala, S.S. Maier, B.C. Simionescu, A.A. Da'dara, P.J. Skelly, C.T. Supuran, Int. J. Mol. Sci. **21**, 1842 (2020)
4. F. Erdemir, D.B. Celepci, A. Aktaş, Y. Gök, R. Kaya, P. Taslimi, Y. Demir, İ Gulçin, Bioorg. Chem. **91**, 103134 (2019)
5. F.A. Bhat, B.A. Ganai, B. Uqab, Asian J. Plant Sci. Res. **7**(3), 17–23 (2017)
6. L. Alaei, R. Khodarahmi, V. Sheikh-Hasani, N. Sheibani, A.A. Moosavi-Movahedi, Int. J. Biol. Macromol. **120**, 1198–1207 (2018)
7. R.J. DiMario, M.C. Machingura, G.L. Waldrop, J.V. Moroney, Plant Sci. **268**, 11–17 (2018)
8. S. Kumar, S. Rulhania, S. Jaswal, V. Monga, Eur. J. Med. Chem. **209**, 112923 (2021)
9. P. Singh, B. Swain, P.S. Thacker, D. Kumar Sigalapalli, P.P. Yadav, A. Angeli, C.T. Supuran, M. Arifuddin, Bioorg. Chem. **99**, 1038392 (2020)
10. S. Akocak, N. Lolak, A. Nocentini, G. Karakoc, A. Tufan, C.T. Supuran, Bioorg. Med. Chem. **25**, 3093–3097 (2017)
11. Z. Afsan, T. Roisnel, S. Tabassum, F. Arjmand, Bioorg. Chem. **94**, 1034272 (2020)
12. V.T. Kasumov, F. Köksal, Spectrochim. Acta Part A **61**, 225–231 (2005)
13. M. Montazerozohori, S. Yadegari, A. Naghiha, S. Veyseh, J. Ind. Eng. Chem. **20**, 118–126 (2014)
14. P. Raghu, T. Madhusudana Reddy, K. Reddaiah, B.E. Kumara Swamy, M. Sreedhar, Food Chem. **142**, 188–196 (2014)
15. I. Bulut, Turk. J. Chem. **33**, 507–520 (2009)
16. K. Gangadhara Reddy, G. Madhavi, B.E. Kumara Swamy, S. Reddy, A. Vijaya Bhaskar Reddy, V. Madhavi, J. Mol. Liq. **180**, 26–30 (2013)
17. M. Emilia Ghica, R.C. Carvalho, A. Amine, C.M.A. Brett, Sens. Actuators B **178**, 270–278 (2013)
18. H. Mohammadi, A. Amine, M. El Rhazi, C.M.A. Brett, Talanta **62**, 951–958 (2004)
19. S. Martic, M. 'Labib, H.-B. Kraatz, Electrochim. Acta **56**, 10676–10682 (2011)
20. I. Bourais, S. Maliki, H. Mohammadi, A. Amine, Enzyme Microb. Technol. **96**, 23–29 (2017)
21. A. Ivanov, R. Davletshina, I. Sharafieva, G. Evtugyn, Talanta **194**, 723–730 (2019)
22. J. Qiu, J. Chen, Q. Ma, Y. Miao, Chemosphere **77**, 129–132 (2009)
23. A.J. Veloso, P.M. Nagy, B. Zhang, D. Dhar, A. Liang, T. Ibrahim, S. Mikhaylichenko, I. Aubert, K. Kerman, Anal. Chim. Acta **774**, 73–78 (2013)
24. S. Gu, Y. Lu, Y. Dinga, L. Li, F. Zhang, Q. Wu, Anal. Chim. Acta **796**, 68–74 (2013)
25. N. Büyükkıdan, B. Büyükkıdan, M. Bülbül, R. Kasımoğulları, S. Mert, J. Enzyme Inhib. Med. Chem. **32**, 208–213 (2017)
26. M. Ul-Hassan, Z.H. Chohan, A. Scozzafava, C.T. Supuran, J. Enzym. Inhib. Med. Chem. **19**(3), 263–267 (2004)
27. D. Canakci, I. Koyuncu, N. Lolak, M. Durgun, S. Akocak, C.T. Supuran, J. Enzym. Inhib. Med. Chem. **34**(1), 110–116 (2018)
28. A. Balaban Gündüzalp, G. Parlakgümüs, D. Uzun, Ü. Ozdemir Ozmen, N. Ozbek, M. Sarı, T. Tunç, J. Mol. Struct. **1105**, 332–340 (2016)
29. Ü. Özdemir Özmen, E. Aktan, F. Ilbiz, A. Balaban Gündüzalp, N. Ozbek, M. Sarı, O. Çelik, S. Saydam, Inorg Chim. Acta **423**, 194–203 (2014)
30. F. Hamurcu, S. Mamaş, Ü. Özmen Özdemir, A. Balaban Gündüzalp, O. Sanlı Senturk, J. Mol. Struct. **1118**, 18–27 (2016)
31. A.J. Downard, Electroanalysis **12**(14), 1085–1096 (2000)
32. A. Adenier, M.M. Chehimi, I. Gallardo, J.N. PinsonVila`, Langmuir **20**, 8243–8253 (2004)
33. A.A. Shaikh, J. Firdaws, B.S. Serajee, M.S. Rahman, P.K. Bakshi, Int. J. Electrochem. Sci. **6**, 2333–2343 (2011)
34. G. Baysal, D. Uzun, E. Hasdemir, J. Electroanal. Chem. **860**, 113893 (2020)
35. G. Ceyhan, M. Köse, V. McKee, S. Urus, A. Gölcü, M. Tümer, Spectrochim. Acta Part A: Mol. Biomol. Spect. **95**, 382–398 (2012)
36. J. Gajdár, K. Tsami, H. Michnová, T. Goněc, M. Brázdová, Z. Soldánová, M. Fojta, J. Jampílek, J. Barek, J. Fischer, Electrochim. Acta **332**, 135485 (2020)
37. A. Balaban Gündüzalp, Ü. Özdemir Özmen, B.S. Çevrimli, S. Mamaş, S. Çete, Med. Chem. Res. **23**, 3255–3268 (2014)

38. M.F.S. Teixeira, M.F. Bergamini, C.M.P. Marques, N. Bocchi, Talanta **63**, 1083–1088 (2004)
39. B. Dinçer, A.P. Ekinci, G. Akyüz, İZ. Kurtoğlu, J. Enzyme Inhib. Med. Chem. **31**, 1662–1665 (2016)
40. C. Temperini, A. Scozzafava, L. Puccetti, C.T. Supuran, Bioorg. Med. Chem. Lett. **15**(23), 5136–5141 (2005)
41. Ü. Özmen Özdemir, F. Arslan, F. Hamurcu, Spectrochim. Acta Part A **75**, 121–126 (2010)
42. L. Stradwick, D. Inglis, J. Kelly, G. Pickering, Flavour **6**(1), 2–8 (2017)
43. Ü. Özmen Özdemir, A. Altuntas, A. Balaban Gündüzalp, F. Arslan, F. Hamurcu, Spectrochim. Acta Part A **128**, 452–460 (2014)
44. A. Ouertani, M. Neifar, R. Ouertani, A.S. Masmoudi, A. Mosbah, A. Cherif, Adv. Tissue Eng. Regen. Med. **5**(2), 85–90 (2019)
45. L. Alaei, R. Khodarahmi, S.-H. Vahid, N. Sheibani, A.M.-M. Ali, Int. J. Biol. Macromol. **120**, 1198–1207 (2018)
46. Y. Yang, B. Unnikrishnan, S. Chen, Int. J. Electrochem. Sci. **6**, 3902–3912 (2011)